Structure-Based Design of Inhibitors of the Aspartic Protease Endothiapepsin by Exploiting Dynamic Combinatorial Chemistry

ARTICLE *in* ANGEWANDTE CHEMIE INTERNATIONAL EDITION · MARCH 2014

Impact Factor: 11.26 · DOI: 10.1002/anie.201309682 · Source: PubMed

8 AUTHORS, INCLUDING:

Milon Mondal
University of Groningen
7 PUBLICATIONS **53** CITATIONS
SEE PROFILE

Constantinos Potamitis
National Hellenic Research Foundation
25 PUBLICATIONS **216** CITATIONS
SEE PROFILE

Maria Zervou
National Hellenic Research Foundation
57 PUBLICATIONS **644** CITATIONS
SEE PROFILE

Anna K H Hirsch
University of Groningen
33 PUBLICATIONS **411** CITATIONS
SEE PROFILE

Enzyme Inhibitors

DOI: 10.1002/anie.201309682

Structure-Based Design of Inhibitors of the Aspartic Protease Endothiapepsin by Exploiting Dynamic Combinatorial Chemistry**

Milon Mondal, Nedyalka Radeva, Helene Köster, Ahyoung Park, Constantinos Potamitis, Maria Zervou, Gerhard Klebe, and Anna K. H. Hirsch**

Abstract: *Structure-based design (SBD) can be used for the design and/or optimization of new inhibitors for a biological target. Whereas de novo SBD is rarely used, most reports on SBD are dealing with the optimization of an initial hit. Dynamic combinatorial chemistry (DCC) has emerged as a powerful strategy to identify bioactive ligands given that it enables the target to direct the synthesis of its strongest binder. We have designed a library of potential inhibitors (acylhydrazones) generated from five aldehydes and five hydrazides and used DCC to identify the best binder(s). After addition of the aspartic protease endothiapepsin, we characterized the protein-bound library member(s) by saturation-transfer difference NMR spectroscopy. Cocrystallization experiments validated the predicted binding mode of the two most potent inhibitors, thus demonstrating that the combination of de novo SBD and DCC constitutes an efficient starting point for hit identification and optimization.*

Over the past decade, dynamic combinatorial chemistry (DCC)[1] has emerged as a powerful strategy to identify ligands for biological targets.[2] DCC allows the formation of a dynamic combinatorial library (DCL), in which the bonds between the building blocks are reversible. Upon addition of a target, one or more library members are bound, thereby leading to selection and amplification of the strongest binders from the DCL. Saturation-transfer difference (STD) NMR spectroscopy, which enables the direct characterization of target—ligand interactions in solution,[3] has been applied to identify DCL members bound to the target.[4] In addition to DCC, structure-based design (SBD) is also a powerful strategy to design and/or optimize bioactive compounds.[5] Whereas de novo SBD is rarely used,[6] most reports on SBD deal with the optimization of an initial hit discovered by other means. Therefore, the combination of SBD and DCC would represent a highly efficient hit-identification strategy in a range of medicinal-chemistry projects. In the present study, we have used de novo SBD in combination with acylhydrazone-based DCC and ^{1}H-STD-NMR spectroscopy to identify a new family of potent hits for endothiapepsin, which belongs to the notoriously challenging class of aspartic proteases.[7] Finally, we have validated the proposed binding mode of the inhibitors by X-ray crystallography.

Endothiapepsin belongs to the family of pepsin-like aspartic proteases, which are involved in a wide range of diseases such as hypertension and malaria.[7] Endothiapepsin has been used as a model enzyme for mechanistic studies[8] as well as for the development of renin[9] and β-secretase[10] inhibitors. Eukaryotic aspartic proteases comprise two structurally similar subunits, each contributing an aspartic acid residue to the catalytic dyad (Asp35 and Asp219 in endothiapepsin) that cleaves the peptide bond of the substrate using a bound water molecule.

The formation of an imine-type bond has been applied to medicinal-chemistry-based DCC projects.[11] In aqueous solution, which is required for any biological application, imines themselves are inherently too unstable. Acylhydrazones, on the other hand, offer the right kinetic and thermodynamic balance.[12] Despite its pH dependence, this type of reversible linkage has started to attract attention.

This linkage requires the target protein to be stable at room temperature for one week (pH 7.2),[2c] the use of aniline as a nucleophilic catalyst (pH 6.2),[13] or an acidic buffer system (pH < 6). Acylhydrazones are attractive for biological DCC given that the building blocks are readily available, afford an amide-type linkage that offers both hydrogen-bond donor and -acceptor sites for molecular recognition by the target and are sufficiently stable both at acidic and physiological pH values (see Figure S1 in the Supporting Information) to enable direct analysis of the DCL. The optimum pH value of endothiapepsin is 4.5, and we have shown that the enzyme is stable under these conditions at room temperature for more than 20 days (see Figure S2 in the Supporting Information), thus making it an ideal target enzyme for an SBD project that exploits acylhydrazone-based DCC.

[*] M. Mondal, Dr. A. K. H. Hirsch
Stratingh Institute for Chemistry, University of Groningen
Nijenborgh 7, 9747 AG Groningen (The Netherlands)
E-mail: A.K.H.Hirsch@rug.nl
Homepage: http://www.rug.nl/research/bio-organic-chemistry/hirsch/

N. Radeva, Dr. H. Köster, Dr. A. Park, Prof. Dr. G. Klebe
Institute of Pharmaceutical Chemistry
Marbacher Weg 6, 35032 Marburg (Germany)
E-mail: Klebe@Staff.Uni-Marburg.de

Dr. C. Potamitis, Dr. M. Zervou
Institute of Biology, Medicinal Chemistry & Biotechnology
National Hellenic Research Foundation
48,Vas. Constantinou Ave, Athens 11635 (Greece)

[**] We thank Pieter van der Meulen for useful suggestions and discussions about STD NMR spectroscopy. Funding was granted by the Netherlands Organisation for Scientific Research (NWO-CW, VENI grant to A.K.H.H.), by the Dutch Ministry of Education, Culture, Science (Gravity program 024.001.035) and European Union's Seventh Framework Programme (FP7-REGPOT-2009-1) under grant agreement no. 245866 (to C.P. and M.Z.), and by the ERC advanced grant no. 268145 DrugProfilBind kindly provided by the EU.

Supporting information for this article is available on the WWW under http://dx.doi.org/10.1002/anie.201309682.

We have used two crystal structures of endothiapepsin (PDB: 3PBD and 3PI0) that represent two alternative binding modes: with and without a crystallographically localized water molecule. We did not use the fragments as a starting point but only the structure of the enzyme.[14] We designed a series of acylhydrazones to address the catalytic dyad through hydrogen-bonding interactions, by using the molecular-modeling software MOLOC[15] and the FlexX docking module in the LeadIT suite.[16] The acylhydrazone moiety appeared to be a suitable central scaffold, as modeling suggested it was anchored to the active site through a strong hydrogen-bond network with the catalytic dyad. We introduced an α-amino group that can form charge-assisted hydrogen bonds to the catalytic dyad as well as to Asp81, Asp33, Gly221, or Thr222. We modeled two alternative

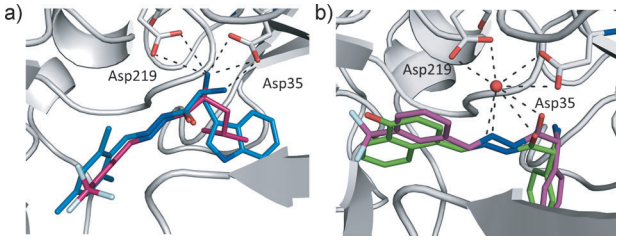

Figure 1. Superposition of MOLOC-generated molecular models of potential inhibitors featuring a) direct hydrogen bonding with the catalytic dyad in the active site of endothiapepsin (PDB code: 3PBD) and b) hydrogen bonding with the catalytic dyad in the active site of endothiapepsin through the catalytic water molecule (PDB code: 3PI0). Color code: protein backbone: gray; inhibitor skeletons: C: green, violet, purple, blue; N: dark blue; F: cyan; O: red; crystallographically localized water molecule: red sphere.

binding poses, in which the acylhydrazone addresses the catalytic dyad either directly or via the catalytic water molecule (Figure 1). During the modeling study, the *E* isomers emerged as the most suitable scaffolds, displaying two vectors pointing towards the S2, S1, S1′, and S2′ pockets. Inspection of the cocrystal structures of endothiapepsin with 11 fragments,[14] as well as hot-spot[17] analyses of the active site of endothiapepsin showed that both aromatic and aliphatic substituents can be accommodated in the S2, S1, S1′, and S2′ pockets surrounding the catalytic dyad. According to our modeling study, both mono- and bicyclic aromatic moieties can be accommodated by the S1′/S2′ pocket, whereas the hydrophobic S2 pocket is best occupied by a mesityl substituent. The S1/S1′ pocket can host an indolyl, isobutyl, or phenyl moiety. We selected a series of acylhydrazone-based inhibitors (see Figure S3 and Table S1 in the Supporting Information for selected docking results), retrosynthesis of which led to five hydrazides **H1**–**H5** and five aldehydes **A1**–**A5** (Scheme 1).

Whereas all the aldehydes as well as hydrazide **H5** are commercially available, hydrazides **H1**–**H4** were obtained in 80–90% yield from their corresponding enantiomerically pure methyl esters by treatment with hydrazine monohydrate (Scheme S1 in the Supporting Information). For the synthesis of hydrazide **H2**, we took advantage of an asymmetric Strecker reaction[18] starting from commercially available *para*-fluorobenzaldehyde (see Scheme S2 in the Supporting Information).

We used ^{1}H-STD-NMR experiments to identify the best component associations bound to endothiapepsin, as this approach enables bound ligands to be monitored and requires only small amounts of unlabeled protein.[3] To facilitate the analysis, we divided the whole library into five sublibraries, each consisting of five hydrazides and one aldehyde, thus resulting in the formation of five potential acylhydrazones (ten isomers, including *E*/*Z* isomers) in equilibrium with the initial building blocks (see Scheme S3 in the Supporting Information). The potential formation of imine products with the free amino group of the hydrazides **H1**–**H4** or a surface-exposed Lys side chain can be ruled out because of the use of acidic conditions.[19] After addition of the target enzyme to the pre-equilibrated libraries, we identified bound acylhydrazones by analyzing the imine-type (see Figures S4, S5, S6, and S7 in the Supporting Information) and α-carbon (see Figure S8 in the Supporting Information) proton signals of acylhydrazones in the ^{1}H-STD-NMR spectra. We identified a total of eight binders from the five sublibraries (Scheme 1).

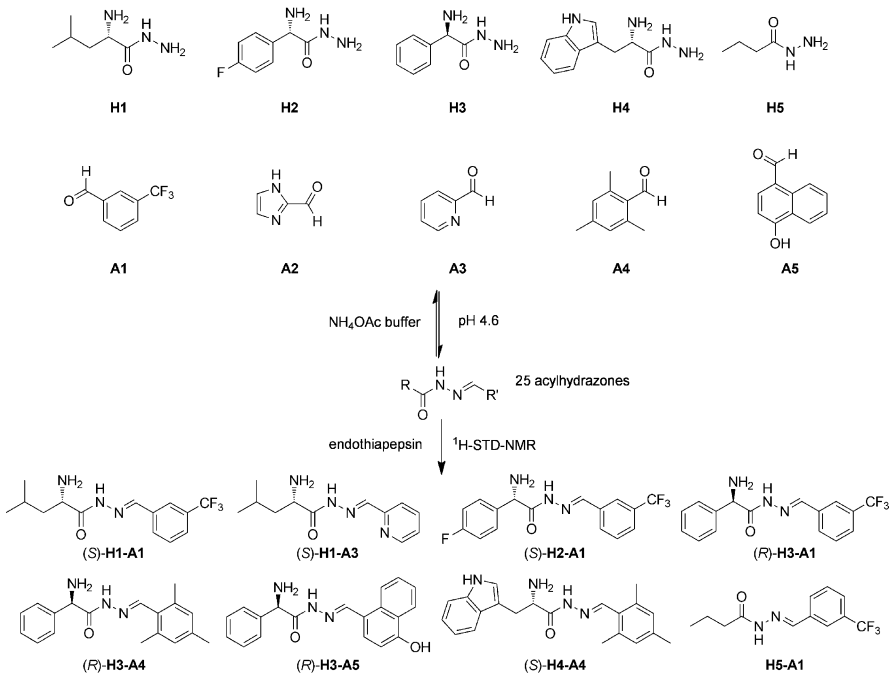

Scheme 1. Dynamic formation of an acylhydrazone library and enzymatic selection of the best inhibitors by ^{1}H-STD-NMR analysis.

To differentiate specific from nonspecific binding, we added the potent inhibitor saquinavir ($K_i = 48$ nM) to the **H1–5 + A4** sublibrary, thereby leading to the appearance of its signals at the expense of the acylhydrazones signals in the ^{1}H-STD-NMR spectrum, thus confirming specific binding of the acylhydrazones **H3-A4** and **H4-A4** (see Figure S9 in the Supporting Information).

To investigate the biological activity of the hits identified by ^{1}H-STD-NMR, we performed inhibition studies using the acylhydrazones (*S*)-**H1-A1**, (*S*)-**H1-A3**, (*S*)-**H2-A1**, (*R*)-**H3-A1**, (*R*)-**H3-A4**, (*R*)-**H3-A5**, (*S*)-**H4-A4**, and **H5-A1** synthesized from their corresponding aldehyde and hydrazide precursors (see Schemes S4 and S5 in the Supporting Information). We determined their inhibitory potency using the mixture of *E*/*Z* isomers by applying a fluorescence-based assay adapted from the HIV-protease assay (see Figures S10—S15 in the Supporting Information).[20]

The enzyme-inhibition assay confirmed the result of the ^{1}H STD NMR experiments. All eight acylhydrazones indeed inhibit endothiapepsin with IC_{50} values in the range of 13 to 365 μM. The most potent inhibitors, acylhydrazones (*S*)-**H4-A4** and (*R*)-**H3-A5**, feature IC_{50} values of 12.8 μM and 14.5 μM, respectively (Table 1). The experimental free energies of binding (ΔG) and ligand efficiencies (LEs), obtained from the IC_{50} values using the Cheng–Prusoff Equation,[21] correlate with the calculated values from the scoring function HYDE in the LeadIT suite (ΔG_{HYDE}((*S*)-**H4-A4**) = −32 kJ mol^{-1}, ΔG_{HYDE} ((*R*)-**H3-A5**) = −26 kJ mol^{-1}; see Table 1 and Table S1 in the Supporting Information).[22]

Table 1: IC_{50} values, calculated K_i values, ΔG values, and LEs of eight acylhydrazones identified as inhibitors of endothiapepsin.[a]

Inhibitor	IC_{50} [μM]	K_i [μM]	ΔG [kJ mol^{-1}]	LE
(*S*)-**H4-A4**	12.8 ± 0.4	6 ± 0.2	−30	0.27
(*R*)-**H3-A5**	14.5 ± 0.5	7 ± 0.2	−30	0.29
(*S*)-**H1-A1**	150 ± 17	71 ± 8	−24	0.27
(*S*)-**H2-A1**	177 ± 13	83 ± 6	−23	0.23
(*R*)-**H3-A4**	206 ± 19	97 ± 9	−23	0.25
(*R*)-**H3-A1**	352 ± 13	166 ± 6	−22	0.22
(*S*)-**H1-A3**	365 ± 95	172 ± 45	−22	0.30
H5-A1	insoluble		–	–

[a] Values indicate the inhibition constant (K_i), the Gibbs free energy of binding (ΔG), and ligand efficiency (LE) derived from the Cheng–Prusoff Equation.[21] Full details of the biological assay conditions are provided in the Supporting Information.

To validate the predicted binding mode from SBD, we soaked crystals of endothiapepsin with the two most potent inhibitors and were able to determine crystal structures of (*R*)-**H3-A5** (PDB code: 3T7P) and (*S*)-**H4-A4** (PDB code: 4KUP) in complex with endothiapepsin at 1.25 Å and 1.31 Å resolution, respectively (see Figures S16—S19 in the Supporting Information). During the soaking experiments, the enzyme selects the *E* isomer from the mixture of *E*/*Z* isomers.

The cocrystal structure of (*R*,*E*)-**H3-A5** shows two ligands in the active site: one binds to the catalytic dyad, whereas the second is oriented towards the solvent. As a result of solvent exposure and lack of protein contacts, the portion of this ligand molecule not visible in the electron density map is most likely highly mobile and scattered over various conformational states. The (*S*,*E*)-**H4-A4** complex also exhibits two ligand molecules in the binding pocket. Of these, only the first binds to the catalytic dyad, whereas the second ligand molecule is solvent-exposed and, by analogy to the previous case, only fractionally visible in the electron density and partially occupied (63 %; Figure 2).

To clarify whether the additional ligands observed are only present because of the high ligand concentrations applied during the soaking, we prepared crystals at different concentrations (2 mM, 20 mM, and 100 mM) and collected separate datasets (PDB codes: 4LHH, 4KUP, and 4LBT). Remarkably, at the lowest concentration, only the binding mode engaging the catalytic dyad is observed. At the highest concentration, population of a third binding pose is apparent (see Figure S20 in the Supporting Information). We therefore believe that only the binding poses of (*R*,*E*)-**H3-A5** and (*S*,*E*)-**H4-A4** next to the catalytic dyad are relevant for our considerations.

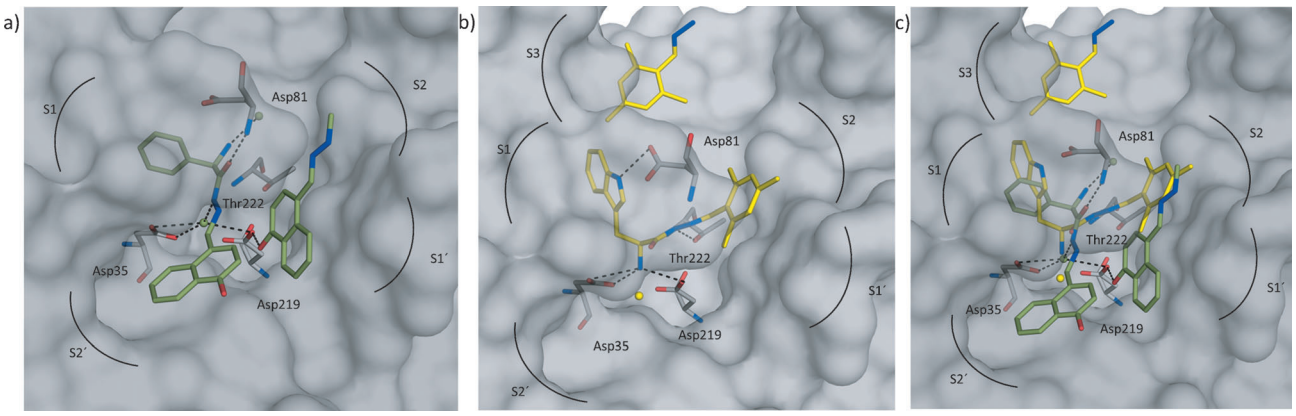

Figure 2. X-ray crystal structures of endothiapepsin cocrystallized with ligands: a) Overview of the two molecules of (*R*,*E*)-**H3-A5** (C: green, water molecules: green spheres) bound in the active site (PDB code: 3T7P). The central ligand binds through the catalytic water molecule to Asp35 and Asp219. b) Overview of both molecules of (*S*,*E*)-**H4-A4** (C: yellow, water molecule: yellow sphere; PDB code: 4KUP). The central ligand addresses Asp35 and Asp219 directly through its α-amino group. c) Superposition of (*R*,*E*)-**H3-A5** and (*S*,*E*)-**H4-A4.** Only the surface of the (*R*,*E*)-**H3-A5** complex is shown.

The detailed binding modes of both ligands are shown in Figure 2 and Figures S11 and S12 in the Supporting Information. The amide NH group of (*R*,*E*)-**H3**-**A5** forms a hydrogen bond to the dyad, mediated by the catalytic water molecule (Figure 2a). The imine-type N atom of the acylhydrazone linker forms a hydrogen bond with the backbone amide NH group of Gly80 (2.9 Å). Another hydrogen bond is observed between the carbonyl group of the acylhydrazone and the backbone amide NH group of Asp81 (3.0 Å). The hydroxy group of the naphtholyl portion of the second ligand donates a hydrogen bond via its hydrogen atom to the outer O atom of the side chain of Asp219 (2.8 Å). Furthermore, the α-amino group of the ligand forms a weak hydrogen bond to an adjacent water molecule, with the remainder of the ligand being bound in the S1′ and S2 pockets and oriented towards the solvent.

(*S*,*E*)-**H4**-**A4** interacts differently with the catalytic dyad (Figure 2b) as it uses its α-amino group to form direct hydrogen bonds to Asp35 (2.8 Å, 3.2 Å) and Asp219 (2.9 Å); the α-amino group occupies virtually the same position as the catalytic water molecule in the complex with (*R*,*E*)-**H3**-**A5**. While the amide-type NH group of the acylhydrazone linker forms a hydrogen bond to the hydroxy group of the Thr222 side chain (2.8 Å), the indolic NH group donates its proton to form a hydrogen bond to the carboxylate group of Asp81 (3.0 Å).

(*R*,*E*)-**H3**-**A5** and (*S*,*E*)-**H4**-**A4** occupy different regions of the binding pocket of endothiapepsin. Clearly, the different binding poses are provoked by the inverted stereochemistry at Cα. This allows (*S*,*E*)-**H4**-**A4** to address the S1 pocket with its indolyl moiety benefiting from CH–π interactions with Phe116 and Leu125 and to form a salt bridge with the catalytic dyad. Furthermore, (*R*,*E*)-**H3**-**A5** places its hydrophobic phenyl group in the S1 pocket and is engaged in CH–π and π–π interactions with Leu125 and Phe116, but its stereochemistry does not allow an interaction with the dyad. Instead the water-mediated contact through its acylhydrazone linker is achieved. This ligand benefits from CH–π interactions with Ile77 and Leu133 through its naphtholyl moiety in the S2′ pocket, whereas (*S*,*E*)-**H4**-**A4** experiences some hydrophobic contacts with Ile300 and Ile304 in the S2 pocket. The binding poses indicated by the additional ligand molecules soaked into the crystals at higher concentrations map out secondary interaction sites most likely experiencing minor affinity contributions.

In conclusion, we have demonstrated for the first time that the combination of de novo SBD and DCC is a powerful technique for the rapid identification of novel hits that inhibit the aspartic protease endothiapepsin. We have exploited ^{1}H-STD-NMR spectroscopy to identify the binders directly from the DCL. Among the hits identified, the best ones exhibit IC_{50} values in the low micromolar range. Subsequent cocrystal-structure determination confirmed our in silico prediction that either direct or water-mediated interactions with the catalytic dyad can be achieved. We have reported the first example of acylhydrazone-based inhibitors of endothiapepsin and aspartic proteases in general. Our synergistic combination of methods holds great promise for the acceleration of the drug-discovery process, not only for the notoriously challenging class of aspartic proteases but for a wide range of drug targets. By enabling the identification and concomitant optimization of novel inhibitors, its potential would appear to be greatest when applied during the early stages of the drug-discovery process.

Received: November 6, 2013
Published online: February 14, 2014

Keywords: dynamic combinatorial chemistry · enzyme inhibitors · STD NMR spectroscopy · structure-based design · X-ray diffraction

[1] a) J.-M. Lehn, *Chem. Soc. Rev.* **2007**, *36*, 151 – 160; b) P. T. Corbett, J. Leclaire, L. Vial, K. R. West, J. Wietor, J. K. M. Sanders, S. Otto, *Chem. Rev.* **2006**, *106*, 3652 – 3711; c) J. Li, P. Nowak, S. Otto, *J. Am. Chem. Soc.* **2013**, *135*, 9222 – 9239.

[2] a) O. Ofori, J. Hoskins, M. Nakamori, C. A. Thornton, B. L. Miller, *Nucleic Acids Res.* **2012**, *40*, 6380 – 6390; b) M. Demetriades, I. K. H. Leung, R. Chowdhury, M. C. Chan, M. A. McDonough, K. K. Yeoh, Y. Tian, T. D. W. Claridge, P. J. Ratcliffe, E. C. Y. Woon, C. J. Schofield, *Angew. Chem.* **2012**, *124*, 6776 – 6779; *Angew. Chem. Int. Ed.* **2012**, *51*, 6672 – 6675; c) V. T. Bhat, A. M. Caniard, T. Luksch, R. Brenk, D. J. Campopiano, M. F. Greaney, *Nat. Chem.* **2010**, *2*, 490 – 497; d) S. Ladame, *Org. Biomol. Chem.* **2008**, *6*, 219 – 226; e) O. Ramström, J.-M. Lehn, *Nat. Rev. Drug Discovery* **2002**, *1*, 26 – 36.

[3] a) J. Angulo, P. M. Nieto, *Eur. Biophys. J.* **2011**, *40*, 1357 – 1369; b) B. Claasen, M. Axmann, R. Meinecke, B. Meyer, *J. Am. Chem. Soc.* **2005**, *127*, 916 – 919; c) S. Di Micco, C. Bassarello, G. Bifulco, R. Riccio, L. Gomez-Paloma, *Angew. Chem.* **2006**, *118*, 230 – 234; *Angew. Chem. Int. Ed.* **2006**, *45*, 224 – 228; d) T. Diercks, J. P. Ribeiro, F. J. Canada, S. Andre, J. Jimenez-Barbero, H. Gabius, *Chem. Eur. J.* **2009**, *15*, 5666 – 5668; e) S. Mari, D. Serrano-Gomez, F. J. Canada, A. L. Corbi, J. Jimenez-Barbera, *Angew. Chem.* **2005**, *117*, 300 – 302; *Angew. Chem. Int. Ed.* **2005**, *44*, 296 – 298; f) B. Meyer, T. Peters, *Angew. Chem.* **2003**, *115*, 890 – 918; *Angew. Chem. Int. Ed.* **2003**, *42*, 864 – 890.

[4] R. Caraballo, H. Dong, J. P. Ribeiro, J. Jimenez-Barbero, O. Ramström, *Angew. Chem.* **2010**, *122*, 599 – 603; *Angew. Chem. Int. Ed.* **2010**, *49*, 589 – 593.

[5] a) A. Kondaskar, S. Kondaskar, J. C. Fishbein, B. A. Carter-Cooper, R. G. Lapidus, M. Sadowska, M. J. Edelman, R. S. Hosmane, *Bioorg. Med. Chem.* **2013**, *21*, 618 – 631; b) S. Kalyaanamoorthy, Y. P. Chen, *Drug Discovery Today* **2011**, *16*, 831 – 839; c) G. Schneider, U. Fechner, *Nat. Rev. Drug Discovery* **2005**, *4*, 649 – 663.

[6] a) A. K. H. Hirsch, S. Lauw, P. Gersbach, W. B. Schweizer, F. Rohdich, W. Eisenreich, A. Bacher, F. Diederich, *ChemMedChem* **2007**, *2*, 806 – 810; b) S. Ni, Y. Yuan, J. Huang, X. Mao, M. Lv, J. Zhu, X. Shen, J. Pei, L. Lai, H. Jiang, J. Li, *J. Med. Chem.* **2009**, *52*, 5295 – 5298.

[7] J. B. Cooper, *Curr. Drug Targets* **2002**, *3*, 155 – 173.

[8] a) L. Coates, P. T. Erskine, S. Mall, R. Gill, S. P. Wood, D. A. A. Myles, J. B. Cooper, *Eur. Biophys. J.* **2006**, *35*, 559 – 566; b) L. Coates, P. T. Erskine, S. P. Wood, D. A. A. Myles, J. B. Cooper, *Biochemistry* **2001**, *40*, 13149 – 13157; c) L. Coates, H. Tuan, S. Tomanicek, A. Kovalevsky, M. Mustyakimov, P. Erskine, J. Cooper, *J. Am. Chem. Soc.* **2008**, *130*, 7235 – 7237.

[9] J. Cooper, W. Quail, C. Frazao, S. I. Foundling, T. L. Blundell, C. Humblet, E. A. Lunney, W. T. Lowther, B. M. Dunn, *Biochemistry* **1992**, *31*, 8142 – 8150.

[10] S. Geschwindner, L. Olsson, J. S. Albert, J. Deinum, P. D. Edwards, T. de Beer, R. H. A. Folmer, *J. Med. Chem.* **2007**, *50*, 5903 – 5911.

[11] G. R. L. Cousins, S. A. Poulsen, J. K. M. Sanders, *Chem. Commun.* **1999**, 1575 – 1576.
[12] a) M. Sindelar, T. A. Lutz, M. Petrera, K. T. Wanner, *J. Med. Chem.* **2013**, *56*, 1323 – 1340; b) M. Hochgürtel, H. Kroth, D. Piecha, M. W. Hofmann, C. Nicolau, S. Krause, O. Schaaf, G. Sonnenmoser, A. V. Eliseev, *Proc. Natl. Acad. Sci. USA* **2002**, *99*, 3382 – 3387; c) T. Bunyapaiboonsri, H. Ramström, O. Ramström, J. Haiech, J.-M. Lehn, *J. Med. Chem.* **2003**, *46*, 5803 – 5811.
[13] A. Dirksen, S. Dirksen, T. M. Hackeng, P. E. Dawson, *J. Am. Chem. Soc.* **2006**, *128*, 15602 – 15603.
[14] H. Köster, T. Craan, S. Brass, C. Herhaus, M. Zentgraf, L. Neumann, A. Heine, G. Klebe, *J. Med. Chem.* **2011**, *54*, 7784 – 7796.
[15] P. R. Gerber, K. Müller, *J. Comput.-Aided Mol. Des.* **1995**, *9*, 251 – 268.
[16] BioSolveIT GmbH, Sankt Augustin. http://www.biosolveit.de, *LeadIT*, version 2.1.3.
[17] H. Gohlke, M. Hendlich, G. Klebe, *Perspect. Drug Discovery Des.* **2000**, *20*, 115 – 144.
[18] Y. Perez-Fuertes, J. E. Taylor, D. A. Tickell, M. F. Mahon, S. D. Bull, T. D. James, *J. Org. Chem.* **2011**, *76*, 6038 – 6047.
[19] C. Godoy-Alcantar, A. K. Yatsimirsky, J.-M. Lehn, *J. Phys. Org. Chem.* **2005**, *18*, 979 – 985.
[20] M. V. Toth, G. R. Marshall, *Int. J. Pept. Protein Res.* **1990**, *36*, 544 – 550.
[21] H. C. Cheng, *J. Pharmacol. Toxicol. Methods* **2001**, *46*, 61 – 71.
[22] a) N. Schneider, S. Hindle, G. Lange, R. Klein, J. Albrecht, H. Briem, K. Beyer, H. Claussen, M. Gastreich, C. Lemmen, M. Rarey, *J. Comput.-Aided Mol. Des.* **2012**, 26, 701 – 723; b) I. Reulecke, G. Lange, J. Albrecht, R. Klein, M. Rarey, *ChemMedChem* **2008**, *3*, 885 – 897.

